Genes & Nutrition

RESEARCH

Open Access

# Impairments in *SHMT2* expression or cellular folate availability reduce oxidative phosphorylation and pyruvate kinase activity

Joanna L. Fiddler[1,2], Jamie E. Blum[1,3], Katarina E. Heyden[1], Luisa F. Castillo[1], Anna E. Thalacker-Mercer[4] and Martha S. Field[1*]

## Abstract

**Background** Serine hydroxymethyltransferase 2 (SHMT2) catalyzes the reversible conversion of tetrahydrofolate (THF) and serine-producing THF-conjugated one-carbon units and glycine in the mitochondria. Biallelic *SHMT2* variants were identified in humans and suggested to alter the protein's active site, potentially disrupting enzymatic function. SHMT2 expression has also been shown to decrease with aging in human fibroblasts. Immortalized cell models of total *SHMT2* loss or folate deficiency exhibit decreased oxidative capacity and impaired mitochondrial complex I assembly and protein levels, suggesting folate-mediated one-carbon metabolism (FOCM) and the oxidative phosphorylation system are functionally coordinated. This study examined the role of SHMT2 and folate availability in regulating mitochondrial function, energy metabolism, and cellular proliferative capacity in both heterozygous and homozygous cell models of reduced *SHMT2* expression. In this study, primary mouse embryonic fibroblasts (MEF) were isolated from a C57Bl/6J dam crossed with a heterozygous *Shmt2*$^{+/-}$ male to generate *Shmt2*$^{+/+}$ (wild-type) or *Shmt2*$^{+/-}$ (HET) MEF cells. In addition, haploid chronic myeloid leukemia cells (HAP1, wild-type) or HAP1 cells lacking SHMT2 expression (ΔSHMT2) were cultured for 4 doublings in either low-folate or folate-sufficient culture media. Cells were examined for proliferation, total folate levels, mtDNA content, protein levels of pyruvate kinase and PGC1α, pyruvate kinase enzyme activity, mitochondrial membrane potential, and mitochondrial function.

**Results** Homozygous loss of *SHMT2* in HAP1 cells impaired cellular folate accumulation and altered mitochondrial DNA content, formate production, membrane potential, and basal respiration. Formate rescued proliferation in HAP1, but not ΔSHMT2, cells cultured in low-folate medium. Pyruvate kinase activity and protein levels were impaired in ΔSHMT2 cells and in MEF cells exposed to low-folate medium. Mitochondrial biogenesis protein levels were elevated in *Shmt2*$^{+/-}$ MEF cells, while mitochondrial mass was increased in both homozygous and heterozygous models of SHMT2 loss.

**Conclusions** The results from this study indicate disrupted mitochondrial FOCM impairs mitochondrial folate accumulation and respiration, mitochondrial formate production, glycolytic activity, and cellular proliferation. These changes persist even after a potentially compensatory increase in mitochondrial biogenesis as a result of decreased SHMT2 levels.

**Keywords** Folate, One-carbon metabolism, SHMT2, Energy metabolism, Oxygen consumption rate, Pyruvate kinase

*Correspondence:
Martha S. Field
mas246@cornell.edu
Full list of author information is available at the end of the article

## Background

Folate coenzymes, found within the folate-mediated one-carbon metabolism (FOCM) metabolic network, mediate the activation and transfer of one-carbon units for diverse cellular processes, including de novo purine and thymidylate (dTMP) biosynthesis, amino acid metabolism, and methionine regeneration [1, 2]. The transfer of one-carbon units is compartmentalized within the nucleus, cytosol, and mitochondria [3], and serine catabolism provides the majority of one-carbon units within mammalian cells [4]. Within the mitochondria, serine hydroxymethyltransferase 2 (SHMT2) catalyzes the reversible conversion of tetrahydrofolate (THF) and serine, producing THF-conjugated one-carbon units and glycine [5]. In this pathway, the majority of serine is converted to formate, which exits the mitochondria and is used in the abovementioned nuclear or cytosolic FOCM processes [1, 6, 7]. Recently, biallelic *SHMT2* variants were identified in humans and suggested to alter the protein's active site [8, 9]. Indeed, patient fibroblasts from individuals with *SHMT2* variants display a decreased ratio of glycine to serine, suggesting disrupted enzymatic function, though the consequences of reduced activity are relatively uncharacterized.

Immortalized/transformed cell models of total *SHMT2* loss have been utilized to study the implications of impaired mitochondrial FOCM. Many of these models have examined the drivers of proliferative capacity in cancer cells, which exhibit higher levels of SHMT2 than noncancer tissue [10, 11]. Interestingly, changes in SHMT2 levels have also been associated with aging; aged human fibroblasts exhibit reduced *SHMT2* expression corresponding with reduced oxygen consumption [12], suggesting SHMT2 not only plays a role in cell proliferation but also in mitochondrial energy metabolism.

Serine-derived one-carbon units can also be used for de novo dTMP biosynthesis within the mitochondria [5, 13]. Mitochondrial DNA (mtDNA) encodes 13 proteins that are required for ATP synthesis as well as mitochondrial tRNA and rRNA molecules, and it has been recognized for decades that mutations in mtDNA increase with age, lead to diseases, and occur ~ 100-fold more frequently than in the nuclear genome [14–16]. Furthermore, reduced *Shmt2* expression and folate deficiency resulted in increased uracil misincorporation in mtDNA, in a heterozygous mouse model of *Shmt2* loss, without affecting uracil misincorporation in the nuclear genome [17]. These findings are consistent with evidence that mtDNA is more sensitive to genomic instability than nuclear DNA [18].

Numerous in vitro studies have focused on the consequences of homozygous loss of *SHMT2* in immortalized/transformed cell; however, in vivo models of homozygous SHMT2 loss are embryonically lethal [17, 19]. *SHMT2* expression also declines with age in human fibroblast cells [12]. Since SHMT2 is at the intersection of aging and cellular proliferation/mitochondrial metabolism, we developed a mouse embryonic fibroblast (MEF) cell model of heterozygous *Shmt2* loss to more closely mimic conditions with reduced SHMT2. Here, we describe the role of SHMT2 and folate availability in regulating energy metabolism and cellular proliferative capacity in heterozygous and homozygous cell models of *SHMT2* expression.

## Results

### Loss of SHMT2 impairs cellular folate accumulation and alters mitochondrial DNA content, membrane potential, and basal respiration in HAP1 cells

We have previously demonstrated that heterozygous *Shmt2*$^{+/-}$ MEF cells exhibited a ~ 50% reduction in SHMT2 protein levels compared to *Shmt2*$^{+/+}$ MEF cells, and *Shmt2*$^{+/+}$ and *Shmt2*$^{+/-}$ MEF cells cultured in low-folate medium had a reduction in total folates [17]. To assess effects of total loss of *SHMT2*, HAP1 cells and *Δ*SHMT2 cells were cultured in medium containing either 25-nM (6S)5-formylTHF (folate-sufficient medium) or 0-nM (6S)5-formylTHF (low-folate medium). The 2-bp deletion in an *SHMT2* coding exon resulted in a significant reduction in SHMT2 protein levels with no visible protein in the *Δ*SHMT2 cells ($p < 0.01$, Fig. 1A). As expected, HAP1 cells and *Δ*SHMT2 cells grown in low-folate medium had impaired accumulation of folate ($p < 0.01$, Fig. 1B), and there was a significant genotype by folate interaction ($p < 0.05$, Fig. 1B). Additionally, *Δ*SHMT2 cells grown in folate-sufficient medium exhibited impaired folate accumulation compared to HAP1 cells grown in folate-sufficient medium ($p = 0.05$, Fig. 1B), consistent with what was observed in *Shmt2*$^{+/-}$ mouse liver mitochondria [17]. To assess cellular uptake and partitioning of folate, HAP1 cells and *Δ*SHMT2 cells were cultured for 26 h in medium containing 25 nM (6RS)-[$^{3}$H]5-formylTHF (folate-sufficient medium). Quantifying cellular tritium levels demonstrated that whole cell and nuclear folate uptake were not significantly different comparing HAP1 and *Δ*SHMT2 cells (Fig. 1C). Mitochondrial folate uptake was not impaired and was elevated in *Δ*SHMT2 cells ($p < 0.05$, Fig. 1C), though as discussed below, and may reflect increased mitochondrial mass in *Δ*SHMT2 cells relative to HAP1 cells.

There were significant genotype by medium interactions in mtDNA content ($p < 0.05$, Fig. 1D) and mitochondrial membrane potential in the HAP1

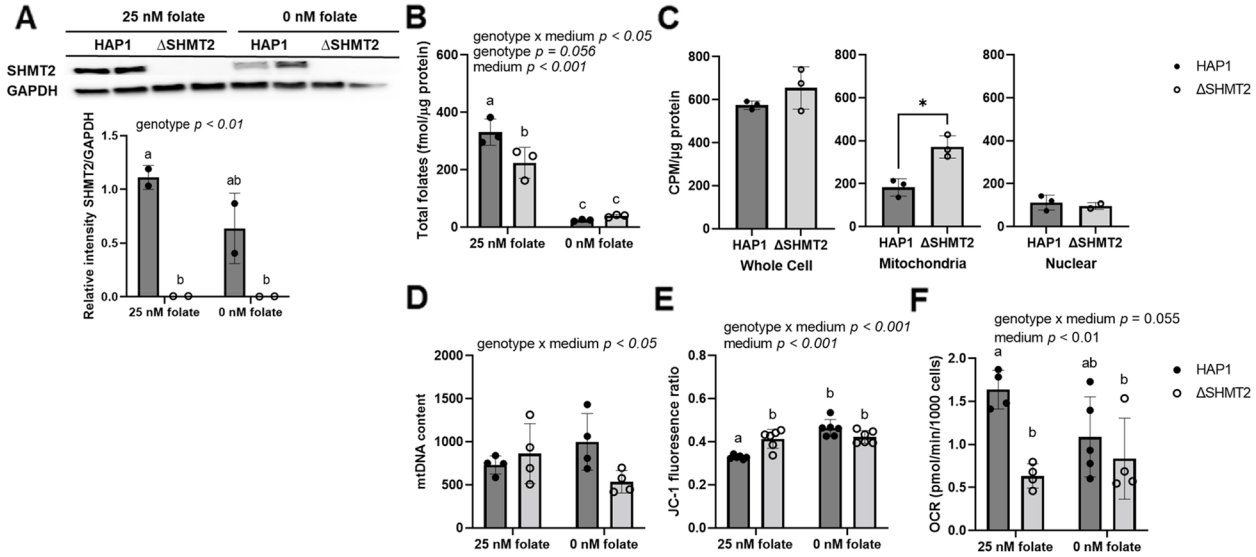


**Fig. 1** Total folates, cellular uptake and particianing of folate, mtDNA content, mitochondrial membrane potential, and basal respirationin HAP1 and ΔSHMT2 cells. Homozygous loss of *SHMT2* and low-folate medium decrease folate accumulation and basal respiration and increase mitochondrial membrane potential in HAP1 cells. **A** SHMT2 protein levels, **B** total folate levels, **C** cellular uptake and partitioning of folate, **D** mtDNA content, **E** mitochondrial membrane potential, and **F** oxygen consumption rate in HAP1 cells and ΔSHMT2 cells. SHMT2 protein levels were normalized to GAPDH, and densitometry was performed using ImageJ. Two-way ANOVA with Tukey's post hoc analysis was used to determine media by genotype interaction and main effects of media and genotype with a statistical significance at $p < 0.05$. Levels not connected by the same letter are significantly different. Data represent means ± SD values, $n = 2$–6 per group. GAPDH, glyceraldegyde-3 phosphate dehydrogenase; SHMT2, serine hydroxymethyltransferase 2

and ΔSHMT2 cells ($p < 0.001$, Fig. 1E). Although the post hoc comparisons indicated no statistical significance between the four groups, mtDNA content in HAP1 cells and ΔSHMT2 cells responded differently to folate availability, with decreased mtDNA content in ΔSHMT2 cells cultured in low-folate medium (Fig. 1D). In addition, exposure to low-folate medium increased mitochondrial membrane potential in both HAP1 and ΔSHMT2 cells ($p < 0.001$, Fig. 1E), and the pairwise comparisons indicate ΔSHMT2 cells cultured in folate-sufficient medium have increased membrane potential compared to the HAP1 cells cultured in folate-sufficient medium. Furthermore, oxygen consumption rate was impaired in ΔSHMT2 cells compared to HAP1 cells; ΔSHMT2 cells cultured in folate-sufficient medium had < 50% less capacity to utilize oxygen than HAP1 cells cultured in folate-sufficient medium ($p < 0.01$, Fig. 1F). A more modest ~ 20% reduction in oxygen consumption was also observed in *Shmt2*$^{+/-}$ MEF cells and in *Shmt2*$^{+/+}$ and *Shmt2*$^{+/-}$ MEF cells cultured in low-folate medium compared to *Shmt2*$^{+/+}$ MEF cells [17]. Additionally, *Shmt2*$^{+/-}$ MEF cells and *Shmt2*$^{+/+}$ and *Shmt2*$^{+/-}$ MEF cells cultured in low-folate medium had decreased mitochondrial membrane potential with no changes in mtDNA content [17].

### Loss of SHMT2 impairs serine-derived one-carbon unit incorporation into formate and impairs cellular proliferation. The addition of formate rescues proliferation in HAP1, but not ΔSHMT2, cells cultured in low-folate medium

We previously demonstrated that *Shmt2*$^{+/-}$ MEF cells and *Shmt2*$^{+/+}$ and *Shmt2*$^{+/-}$ MEF cells cultured in low-folate medium had reduced cellular proliferation, and the addition of 2-mM formate restored cellular proliferation in *Shmt2*$^{+/+}$ and *Shmt2*$^{+/-}$ MEF cells cultured in low-folate medium [17]. Examination of cell proliferation rates with total loss of *SHMT2* confirmed significant effects of ΔSHMT2 genotype, exposure to low-folate media, and medium over time interaction for the cell proliferation ($p < 0.001$ for all main effects and interactions; Fig. 2A). The genotype-driven differences in cell proliferation were significant at day 1 and became more pronounced at days 2 and 3 (Fig. 2B). The addition of 2-mM formate rescued growth of HAP1 cells cultured in low-folate medium, but not ΔSHMT2 cells in either medium type (Fig. 2A and C). This finding suggests that mitochondrial conversion of one-carbon units from serine to formate is not the only growth-limiting effect of *SHMT2* loss. Interestingly, 2-mM formate supplementation enhanced the proliferation capacity of HAP1 cells culture in low-folate medium compared to HAP1 cells cultured in folate-sufficient medium at

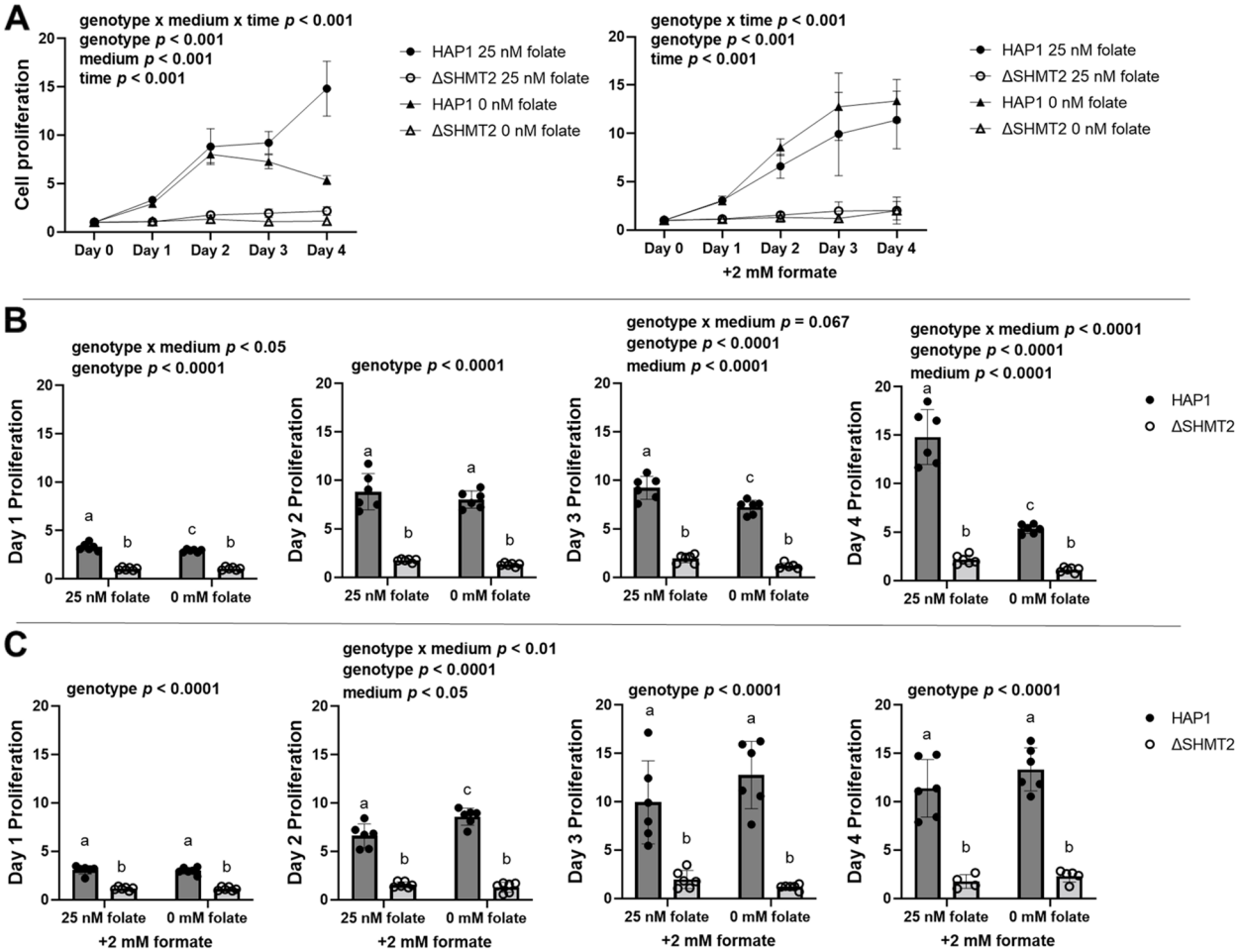


**Fig. 2** Cellular proliferation rates in HAP1 and ΔSHMT2 cells. Formate rescues cell proliferation rate in HAP1 cells cultured in low-folate medium but not in ΔSHMT2 cells. Cell proliferation rates of ΔSHMT2 cells were compared with HAP1 cells by co-staining cells with Hoechst 33342 (to identify all cells) and propidium iodide (to identify dead cells). Fold change of each group was calculated by dividing by day 0 cell number. Data represent means ± SD values. Values represent $n = 6$ replicates of cell lines cultured in medium containing either 25 nM (6S)5-formyl-THF or 0 nM (6S)5-formyl-THF. **A** Cell proliferation rate and cell proliferation rate in the presence of 2 mM formate, **B** relative days 1–4 quantitation of cell proliferation rate, and **C** relative days 1–4 quantitation cell proliferation rate in the presence of 2-mM formate. Linear mixed-effects models with main effects of media, genotype, and time (with time as a continuous variable) and 2- and 3-way interactions were used to determine cell proliferation with a statistical significance at $p < 0.05$. Two-way ANOVA with Tukey's post hoc analysis was used to determine media by genotype interaction and main effects of media, and genotype with a statistical significance at $p < 0.05$ were used to analyze individual day proliferation. Levels not connected by the same letter are significantly different

day 2, but the difference was lost by days 3 and 4 (Fig. 2C). ΔSHMT2 cells cultured in folate-sufficient IMDM medium had reduced cellular proliferation compared to HAP1 cells (Fig. S1 A–B); furthermore, the addition of formate also failed to rescue the impaired proliferation even in what is considered "complete" culture medium for HAP1 cells (Fig. S1 A–B). To assess the contribution of serine one-carbon units for de novo dTMP synthesis, HAP1 cells and ΔSHMT2 cells were cultured in 25- or 0-nM (6S)5-formylTHF containing $_{L}$-[2,3,4-$^{2}H_{3}$]-serine until confluency. The relative contribution of $_{L}$-[2,3,4-$^{2}H_{3}$]-serine contributing to dTMP synthesis from formate, represented by the D1/D1 + D2 ratio, was reduced by ~ 60% in ΔSHMT2 cells cultured in folate-sufficient medium and by ~ 55% in HAP1 cells cultured in low-folate medium (Fig. 3).

## Glycolytic and mitochondrial biogenesis protein levels and ATP production exhibit distinct responses in cell models of homozygous and heterozygous SHMT2 expression

Heterozygous disruption of *Shmt2* expression in MEF cells [17] and ΔSHMT2 cells exhibit impaired oxygen consumption (Fig. 1); therefore, to determine if glycolytic activity was increased to compensate for the

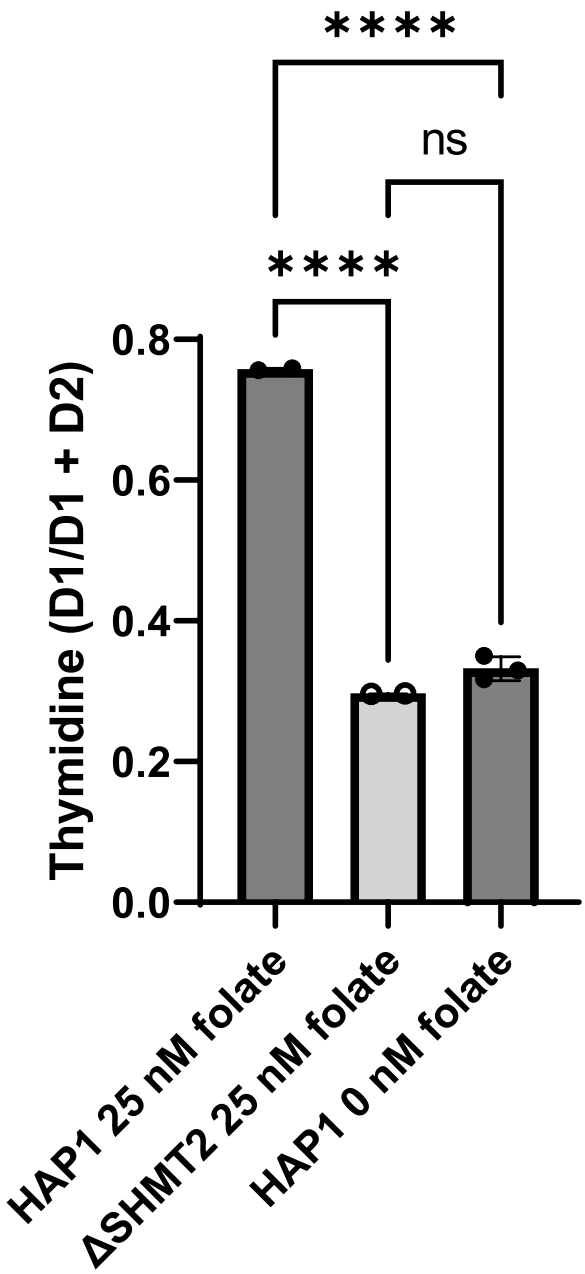


**Fig. 3** Contribution of serine one-carbon units for de novo dTMP synthesis. $_{L}$-[2,3,4-$^{2}H_{3}$]-serine contribution to dTMP synthesis from formate was reduced with homozygous loss of SHMT2 and in HAP1 cells cultured in low-folate medium compared to HAP1 cells culture in folate-sufficient medium. One-way ANOVA with Tukey's post hoc analysis was used with a statistical significance of $p < 0.05$. Data represents means ± SD values, $n = 2–3$ per group. $_{L}$-[2,3,4-$^{2}H_{3}$]-serine incorporation into thymidine is conveyed by the ratio of carbons containing one deuterium atom/total number of carbons containing one and two deuterium atoms

reduction in ATP generation from oxidative phosphorylation, we assayed pyruvate kinase activity. Protein levels of PKM1 and PKM2 were significantly reduced in ΔSHMT2 cells compared to HAP1 cells ($p < 0.01$; Fig. 4A). Interestingly, protein levels of PKM1 and PKM2 in *Shmt2*$^{+/+}$ and *Shmt2*$^{+/-}$ MEF cells were reduced only when the cells were cultured in low-folate medium, with more robust changes in PKM1 protein levels compared to PKM2 protein levels as a result of exposure to low-folate medium (Fig. 5A). Pyruvate kinase enzyme activity corresponded with the proteins levels; activity was significantly reduced in ΔSHMT2 cells compared to HAP1 cells ($p < 0.001$ for genotype and genotype by medium interaction; Fig. 4B) and in both *Shmt2*$^{+/+}$ and *Shmt2*$^{+/-}$ MEF cells cultured in low-folate medium ($p < 0.001$; Fig. 5B). Because oxygen consumption and pyruvate kinase protein levels and enzyme activity were impaired in both cell models, we evaluated ATP production and extracellular acidification rates (ECAR). ATP production was significantly reduced in ΔSHMT2 cells compared to HAP1 cells ($p < 0.001$; Fig. 6A) and in both *Shmt2*$^{+/+}$ and *Shmt2*$^{+/-}$ MEF cells cultured in low-folate medium ($p < 0.05$; Fig. 6B). Interestingly, *Shmt2*$^{+/-}$ MEF cells cultured in folate-sufficient medium exhibited a reduced ATP production compared to folate-sufficient *Shmt2*$^{+/+}$ MEF cells (Fig. 6B). Furthermore, both cell models of *SHMT2* loss had reduced ECAR rates compared to the wild-type cells (Fig. 6C and D). In addition, MEF cells exposed to low-folate medium displayed reduced ECAR rates compared to MEF cells grown in folate-sufficient medium (Fig. 6D). To determine if mitochondrial biogenesis was impacted in these models, we examined protein levels of the transcription factor PPARG coactivator *1 alpha* (PGC1α). *Shmt2*$^{+/-}$ MEF cells cultured in folate-sufficient medium exhibited a 16-fold increase in PGC1α protein levels compared to *Shmt2*$^{+/+}$ MEF cells (Fig. 5A). PGC1α protein was not detected in HAP1 cells or ΔSHMT2 cells (data not shown).

#### Mitochondrial mass is increased as a result of homozygous and heterozygous SHMT2 deletion, while NAD/NADH ratio is reduced only with homozygous loss of SHMT2

To further evaluate markers of mitochondrial health and metabolism in the homozygous and heterozygous *SHMT2* cell models, citrate synthase activity and NAD/NADH ratio were measured. Citrate synthase activity (a biomarker for mitochondrial mass [20]) was significantly increased in both ΔSHMT2 cells ($p < 0.001$; Fig. 7A) and *Shmt2*$^{+/-}$ MEF cells ($p < 0.05$; Fig. 7B) compared to their respective wild-type cells. Additionally, there was a genotype by medium interaction in HAP1 cells and ΔSHMT2 cells cultured in low-folate and folate-sufficient medium (Fig. 7A). Levels of NAD/NADH in ΔSHMT2 cells were modestly reduced by 17% compared to HAP1 cells ($p < 0.05$; Fig. 8A). There were no differences in NAD/

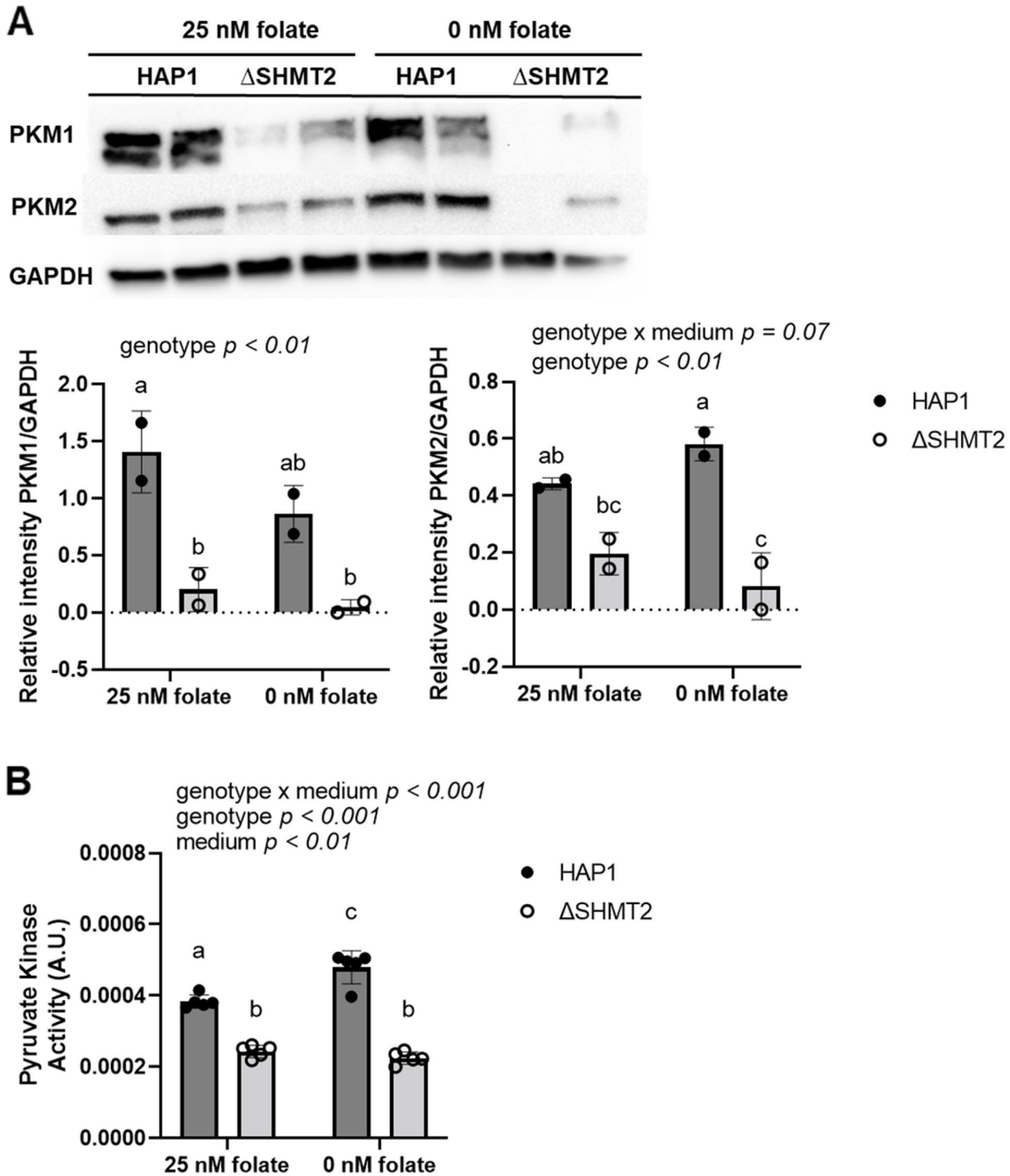


**Fig. 4** Protein levels and pyruvate kinase activity in HAP1 and ΔSHMT2 cells. Homozygous loss of *SHMT2* reduces protein levels and activity of pyruvate kinase in HAP1 cells. **A** PKM1 and PKM2 protein levels and **B** pyruvate kinase activity in HAP1 cells and ΔSHMT2 cells. PKM1 and PKM2 protein levels were normalized to GAPDH, and densitometry was performed using ImageJ. Two-way ANOVA with Tukey's post hoc analysis was used to determine media by genotype interaction and main effects of media and genotype with a statistical significance at $p < 0.05$. Levels not connected by the same letter are significantly different. Data represent means ± SD values, $n = 2$–5 per group. GAPDH, glyceraldegyde-3 phosphate dehydrogenase; PKM1 and PKM2, pyruvate kinase M1 and M2 isoforms

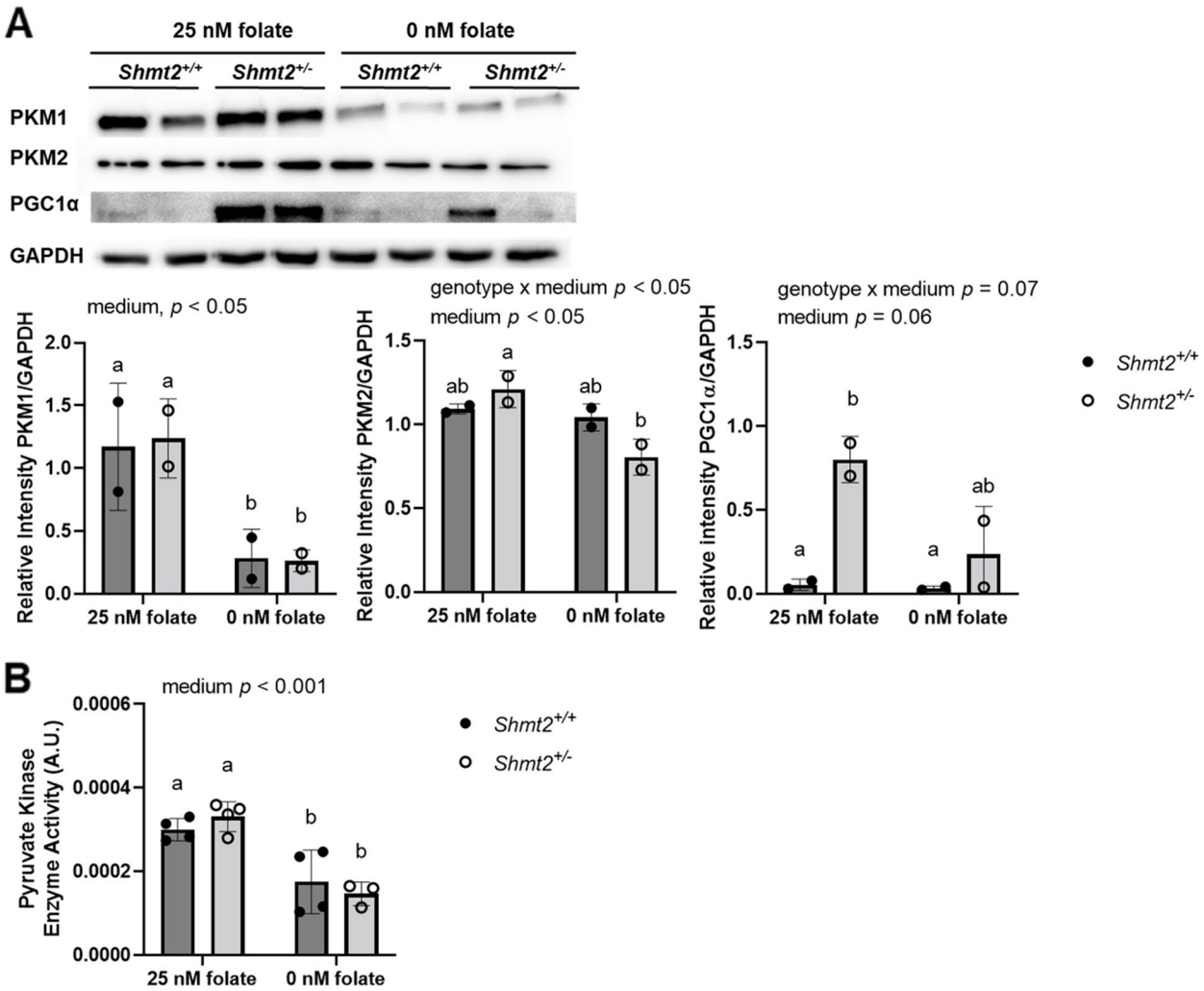


**Fig. 5** Protein levels and pyruvate kinase activity inShmt2$^{+/+}$ and *Shmt2*$^{+/-}$ MEF cells. Low-folate medium decreases protein levels, and activity of pyruvate kinase in MEF cells and reduced *Shmt2* expression increases PGC1α protein levels. **A** PKM1, PKM2, and PGC1α protein levels and **B** pyruvate kinase activity in *Shmt2*$^{+/+}$ and *Shmt2*$^{+/-}$ MEF cells. PKM1, PKM2, and PGC1α protein levels were normalized to GAPDH, and densitometry was performed using ImageJ. Two-way ANOVA with Tukey's post hoc analysis was used to determine media by genotype interaction and main effects of media and genotype with a statistical significance at $p < 0.05$. Levels not connected by the same letter are significantly different. Data represent means ± SD values, $n = 2$–4 per group with 2 embryo cells lines represented in each group. GAPDH, glyceraldegyde-3 phosphate dehydrogenase; PGC1α, PPARγ coactivator-1α; PKM1 and PKM2, pyruvate kinase M1 and M2 isoforms

NADH comparing *Shmt2*$^{+/+}$ and *Shmt2*$^{+/-}$ MEF cells (Fig. 8B).

## Discussion

With the identification of biallelic *SHMT2* human variants [8] and the observation that *SHMT2* expression in human fibroblasts is decreased with age [12], understanding the cellular implications of perturbed mitochondrial FOCM is of great interest. In *Δ*SHMT2 cells, we observed decreased total folate accumulation, which is consistent with our previous finding that *Shmt2*$^{+/-}$ liver mitochondria accumulate 25% less folate than liver mitochondria from *Shmt2*$^{+/+}$ mice even when consuming adequate dietary folate [17]. Interestingly, mitochondrial folate uptake in *Δ*SHMT2 cells was not impaired (Fig. 1C), and the apparent increase in mitochondrial folate uptake in *Δ*SHMT2 cells paralleled the increase in mitochondrial mass observed in ΔSHMT2 cells compared to HAP1 cells (Fig. 7A). The intracellular concentration of folate-utilizing enzymes is higher than the concentration of intracellular folate cofactors, which creates competition for a limited amount of cofactor and indicates that intracellular folate cofactors are protein bound [21]. Since mitochondria contain approximately

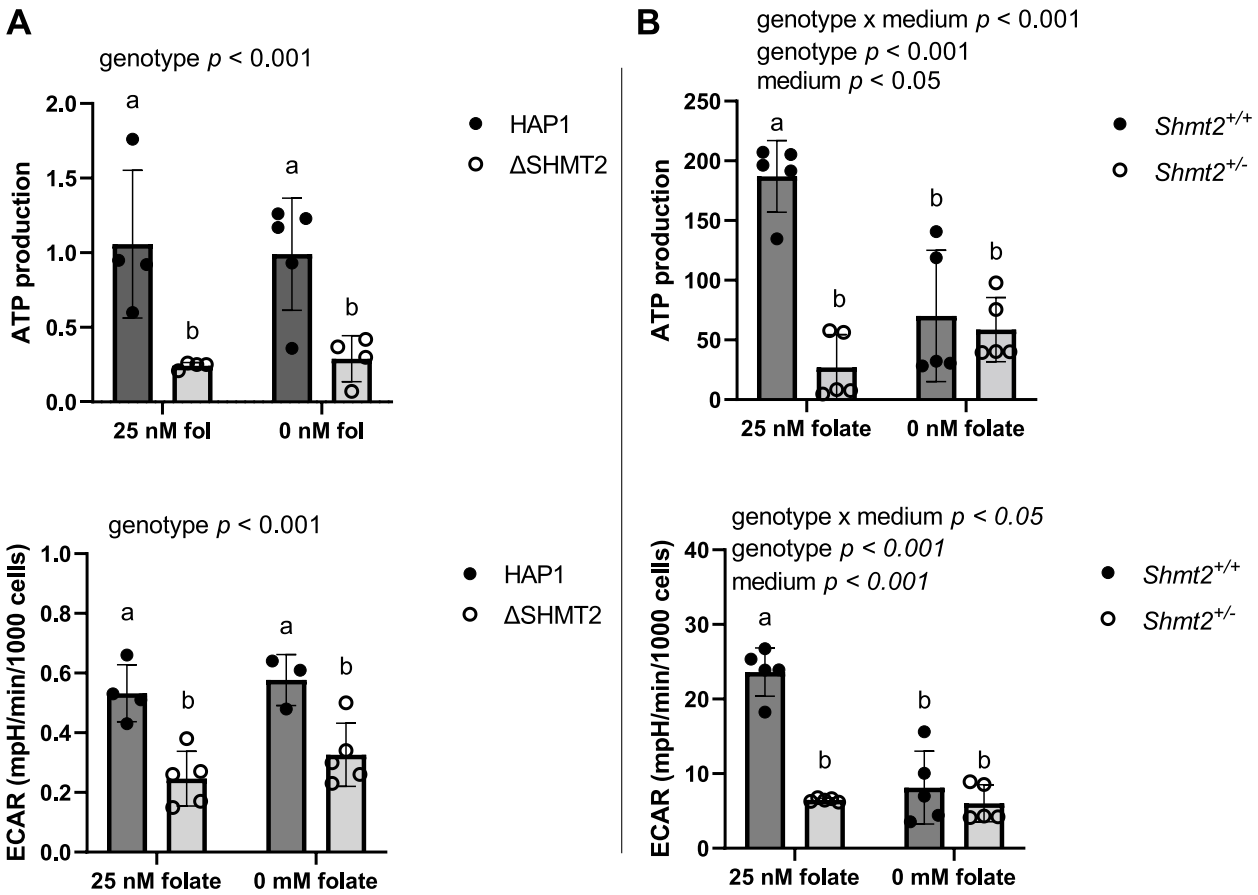


**Fig. 6** Cell type ATP production and extracellular acidification rates. Decreased SHMT2 and exposure to low-folate medium impair ATP production and ECAR. ATP production and extracellular acidification rates in **A** HAP1 cells and ΔSHMT2 cells and **B** $Shmt2^{+/+}$ and $Shmt2^{+/-}$ MEF cells. ATP production and extracellular acidification rates were normalized to total cell count. Two-way ANOVA with Tukey's post hoc analysis was used to determine media by genotype interaction and main effects of media and genotype with a statistical significance at $p < 0.05$. Levels not connected by the same letter are significantly different. Data represent means ± SD values, $n = 4$ per group with 2 embryo cells lines represented in each group

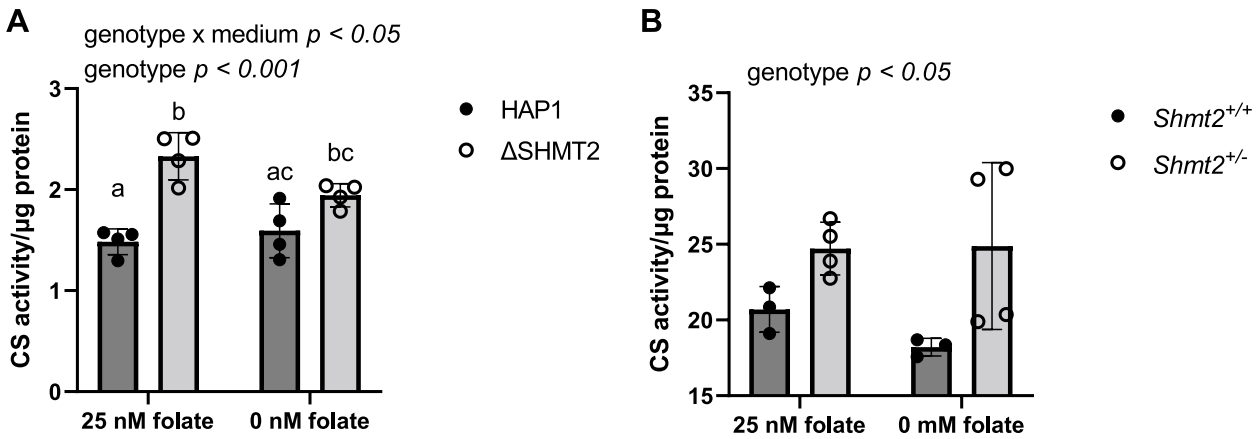


**Fig. 7** Cell type responses in mitochondrial mass. Decreased SHMT2 leads to increased mitochondrial mass. Citrate synthase activity in **A** HAP1 cells and ΔSHMT2 cells and **B** $Shmt2^{+/+}$ and $Shmt2^{+/-}$ MEF cells. Citrate synthase activity was normalized to total protein. Two-way ANOVA with Tukey's post hoc analysis was used to determine media by genotype interaction and main effects of media and genotype with a statistical significance at $p < 0.05$. Levels not connected by the same letter are significantly different. Data represent means ± SD values, $n = 4$ per group with 2 embryo cells lines represented in each group. CS, citrate synthase

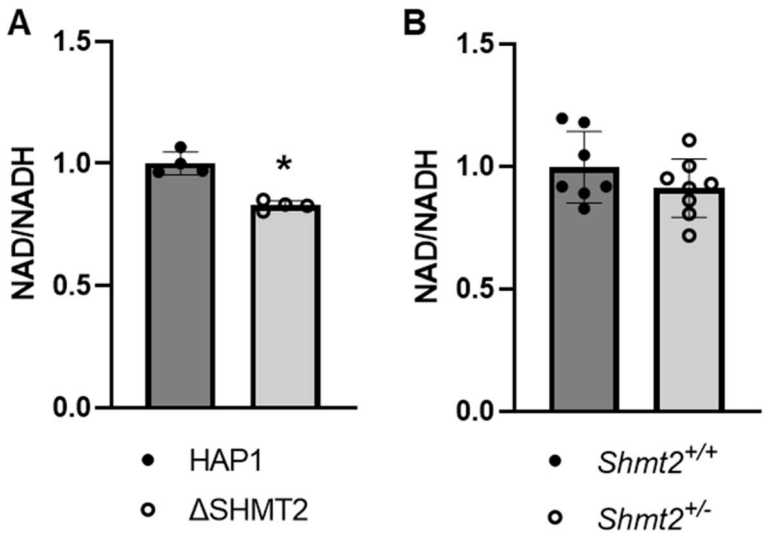


**Fig. 8** Cell type responses in NAD/NADH ratio. NAD/NADH ratio is impaired with homozygous *SHMT2* loss but not heterozygous loss. NAD/NADH ratio in **A** HAP1 cells and ΔSHMT2 cells and **B** $Shmt2^{+/+}$ and $Shmt2^{+/-}$ MEF cells. NAD/NADH ratio was normalized to total cell count. Student's *t*-test was used to determine genotype effects with a statistical significance (*) at $p < 0.05$. Data represent means ± SD values, $n = 4–8$ per group with 2 embryo cells lines represented in each group for the MEF cell analyses

40% of total cellular folate [3], the decreased whole-cell total folate level in ΔSHMT2 cells likely reflects impaired mitochondrial folate accumulation as a result of *Shmt2* loss.

Effects of SHMT2 loss on cellular proliferation have varied by cell type. Multiple homozygous *SHMT2* deletion cell models indicate there are no changes in cellular proliferation rates compared to wild-type cells [22, 23]. We previously demonstrated heterozygous *Shmt2* MEF cells have impaired proliferative capacity [17]. Further supporting the distinct cell type response with *SHMT2* loss, ΔSHMT2 cells cultured in either a low-folate modified medium or the more favorable IMDM medium (Figs. 2 and S1) have impaired proliferative capacity compared to HAP1 cells cultured in the same media. The proliferative capacity and respiratory defects were not rescued by the addition of glycine in heterozygous *Shmt2* expressing MEF cells [17] or in ΔSHMT2 cells, as their growth medium contained adequate glycine levels. This suggests the one-carbon groups entering the folate pool from the glycine cleavage system are not sufficient to overcome the loss of serine-derived one-carbon units from the mitochondria to support cellular proliferation or mitochondrial function. The contribution of one-carbon units from serine to the production of formate in the mitochondria is reduced in ΔSHMT2 cells cultured in folate-sufficient medium and HAP1 cells cultured in low-folate medium (Fig. 3). Formate supplementation rescued HAP1 cell proliferation in cells cultured in low-folate medium (Fig. 2) [17]. The inability of formate supplementation to rescue impaired proliferation in ΔSHMT2 cells suggests that the impact of SHMT2 loss on proliferation is due to effects of SHMT2 other than simply providing formate for nuclear/cytosolic FOCM, as has been suggested in other cell models [24], including in MEF cells [17].

PKM has two isoforms, PKM1 and PKM2; PKM1 is expressed in differentiated tissues (i.e., brain and muscle), while PKM2 is expressed in cancer cells, embryonic cells, and in proliferating cells [25, 26]. It has previously been proposed that PKM1 promotes oxidative phosphorylation [27] and proliferation arrest due to a reduction in nucleotide biosynthesis [28], while silencing of PKM1 impairs mitochondrial membrane potential and induces apoptosis [27]. PKM2 activity was upregulated in cancer cells with experimentally suppressed *SHMT2* expression [22], suggesting that lower levels of SHMT2 promote PKM2-mediated production of pyruvate and ATP, which ultimately supports cell proliferation. This is supported by the recent evidence prostate cancer cell proliferation is dependent on the downregulation of *SHMT2* [29]. Conversely, we found that ΔSHMT2 cells had substantially reduced protein levels of PKM1 and PKM2 and reduced PK activity relative to HAP1 cells (Fig. 4A and B). Independent of *Shmt2* expression levels, MEF cells exposed to low-folate medium had severely reduced protein levels of PKM1 and PK activity, with a modest reduction in PKM2 protein levels (Fig. 5 A and B). To our knowledge, this is the first observation of an effect of decreased cellular folate availability on PK activity. In addition, it does not

appear that glycolysis or lactate/hydrogen ion production is adequately increased to compensate for the reduction in mitochondrial respiration in either cell model, as both ATP production and ECAR were decreased with loss of SHMT2 or folate-depletion (Fig. 6A–D). This is also supported by other cell models of SHMT2 loss that indicate the rate-limiting glycolytic proteins, hexokinase and phosphofructokinase, are unchanged with loss of SHMT2 [23]. In addition to the reduction in glycolytic and respiratory capacity, it has also been demonstrated that the TCA cycle intermediates citrate, succinate, malate, and aspartate are lower in cells with homozygous loss of SHMT2 [30]. The reduced ATP production may influence the impaired proliferative capacity exhibited in *Δ*SHMT2 cells, *Shmt2*$^{+/-}$ MEF cells, and MEF cells exposed to low-folate medium. Of note, there were low cell death rates after exposure to low-folate medium (< 5%, data not shown).

Immortalized/transformed and MEF cell models of homozygous loss of *SHMT2* indicate mitochondrial-derived protein levels and respiratory capacity are severely impaired; however, there were no changes in mRNA levels of these genes [19, 23, 31]. This supports the findings from immortalized/transformed cell models of total *SHMT2* loss that suggest reduced respiratory capacity results from impaired mitochondrial translation [30, 32]. Interestingly, both *Δ*SHMT2 cells and *Shmt2*$^{+/-}$ MEF cells have increased mitochondrial mass (Fig. 7 A and B), suggesting increased mitochondrial number in an attempt to compensate for reduced mitochondrial function. The inability to correct the impaired mitochondrial function could be from uracil misincorporation in mtDNA, as exhibited in *Shmt2*$^{+/-}$ mice or *Shmt2*$^{+/+}$ mice exposed to low-folate diet for 7 weeks [17], potentially causing genomic instability. The mitochondrial mass in both cell types was increased in response to loss of SHMT2; however, the overall mitochondrial mass in HAP1-derived cells was much lower than in MEF cells. Another compensatory response that was only observed in *Shmt2*$^{+/-}$ MEF cells was increased PGC1α protein levels. PGC1α is a transcription factor known to stimulate mitochondrial biogenesis [33, 34]. The robust increase in PGC1α protein levels in *Shmt2*$^{+/-}$ MEF cells is consistent with increased mitochondrial biogenesis and suggests cells with heterozygous loss of *Shmt2* may be attempting to compensate for the impaired mitochondrial function with increased mitochondrial mass (Fig. 7B). Furthermore, homozygous loss of *Shmt2* decreased the NAD/NADH ratio by a modest 20% (Fig. 8A). Such decreased NAD/NADH indicates an accumulation of NADH, which has been observed more robustly in other immortalized cell models of homozygous *Shmt2* loss and associated oxidative phosphorylation impairment [30, 35]. Importantly, there were no changes in NAD/NADH ratio in the heterozygous *Shmt2* MEF cells (Fig. 7B). Taken together, both homozygous and heterozygous models of *Shmt2* loss within suggest the impairments exhibited in oxidative phosphorylation are not a result of substantial NADH accumulation.

The findings presented here support the notion that SHMT2 and adequate folate are essential for mitochondrial function and may have important implications for older adults, as *SHMT2* expression in human fibroblasts declines with age [12]. These data also indicate that there are tissue-specific responses to reduced SHMT2 protein levels. Taken together, understanding age-associated changes in *SHMT2* expression levels, and investigating tissue-specific changes in response to reduced *SHMT2*, should be assessed in future work.

## Conclusions

In this study, heterozygous and homozygous cell models of *SHMT2* expression exposed to low or adequate levels of folate were investigated. The results demonstrate that disrupted mitochondrial FOCM impairs mitochondrial folate accumulation and respiration, mitochondrial formate production, pyruvate kinase activity, and cellular proliferation. These findings provide evidence for the essentiality of SHMT2 and folate in maintaining energy production and have important implications for individuals with SHMT2 variants and in aging individuals.

## Methods

### Cell culture conditions

HAP1 cells (wild-type) and SHMT2 knockout HAP1 (*Δ*SHMT2) cells were obtained from Horizon Discovery: *Δ*SHMT2 cells were generated by Horizon Discovery using CRISPR/Cas9 and contain a 2-bp deletion in SHMT2 coding exon 2. HAP1 cells are a near-haploid cell line that was derived from human chronic myelogenous leukemia cell line KBM-7. Validity of the *Δ*SHMT2 cell line was confirmed by PCR amplification and Sanger sequencing. Cells were regularly passaged in Iscove's Modification of DMEM (IMDM; Corning) supplemented with 10% FBS and 1% penicillin/streptomycin until exposure to folate-sufficient and folate-deficient experimental conditions. Because metabolism-related phenotypes often do not manifest based on nutrient availability, we cultured HAP1 and *Δ*SHMT2 cells for four doublings in 25-nM (folate-sufficient) and 0-nM (folate-deficient) folate supplemented modified DMEM medium (HyClone; formulated to lack glucose, glutamine, B vitamins, methionine, glycine, and serine) containing 10% fetal bovine serum, 1% penicillin/streptomycin, 4.5 g/L glucose, 3 g/L sodium bicarbonate, 4-nM glutamine, 200-μM methionine, 4 mg/L pyridoxine,

30 mg/L glycine, and 25- or 0-nM (6S)-5-formyl-THF. The HAP1 and *Δ*SHMT2 cells were not viable in dialyzed FBS; therefore, non-dialyzed FBS was supplemented in the medium. Total folates (described below) were determined to confirm lower folate levels in cells cultured in 0 nM (6S)-5-formyl-THF.

Mouse embryonic fibroblasts were isolated from C57Bl/6 J female mice bred to *Shmt2*$^{+/-}$ male mice as previously described [17]. All experiments include wild-type *Shmt2*$^{+/+}$ and heterozygous *Shmt2*$^{+/-}$ MEF cells. Cells were regularly passaged in alpha-minimal essential medium (alpha-MEM; HyClone Laboratories) supplemented with 10% FBS and 1% penicillin/streptomycin. For 25- and 0-nM folate supplemented experimental conditions, cells were cultured in modified alpha-MEM (HyClone; lacking glycine, serine, methionine, B vitamins, and nucleosides); modified alpha-MEM was supplemented with 10% dialyzed FBS, 200-μM methionine, 1 mg/L pyridoxine, and 25- or 0-nM (6S)-5-formyl-THF.

#### Cell proliferation

HAP1 cells and *Δ*SHMT2 cells were seeded at 1000 cells per well in 96-well plates in 25-nM and 0-nM folate supplemented medium with the addition of 0- or 2-mM formate. The number of total and dead cells was determined at specified time points by co-staining cells with Hoechst 33,342 (Life Technologies) and propidium iodide (Thermo Fisher Scientific), respectively. Cells were visualized and quantified using a Celigo imaging cytometer (Nexcelom) following the manufacturer's instructions. The number of live cells was determined by subtracting the number of propidium iodide-positive cells from the Hoechst 33,342-positive cells. Data are shown as cell proliferation normalized to cell number on day 1.

#### Immunoblotting

Total protein was extracted following tissue lysis by sonication in lysis buffer (150-mM NaCl, 5-mM EDTA pH8, 1% Triton X-100, 10-mM Tris–Cl, 5-mM dithiothreitol, and protease inhibitor) and quantified by the Lowry-Bensadoun assay [36]. Proteins were denatured by heating with 6 × Laemmeli buffer for 5 min at 95 °C. Samples were electrophoresed on 8–12% SDS-PAGE gels for approximately 60–70 min in SDS-PAGE running buffer and then transferred to an Immobilon-P polyvinylidene difluoride membrane (Millipore Corp.) using a Mini Trans-Blot apparatus (Bio-Rad). Membranes were blocked in 5% (w/v) nonfat dairy milk in 1 × TBS containing 0.1% Tween-20 for 1 h at room temperature. The membranes were incubated overnight in the primary antibody at 4 °C and then washed with 1 × TBS containing 0.1% Tween-20 and incubated with the appropriate horseradish peroxidase-conjugated secondary antibody at 4 °C for 1 h at room temperature. The membranes were visualized with Clarity and Clarity Max ECL Western Blotting Substrates (Bio-Rad). Antibodies against SHMT2 (cell signaling, 1:1000), PKM1 (cell signaling, 1:1000), PKM2 (cell signaling, 1:1000), PGC1α (cell signaling, 1:1000), and GAPDH (cell signaling, 1:2000) were used. For antibody detection, a goat anti-rabbit IgG-horseradish peroxidase-conjugated secondary (Pierce) was used at a 1:15,000 dilution. Membranes were imaged using FluorChem E (Protein Simple), and densitometry was performed with ImageJ (version 1.53a) using GAPDH as the control.

#### Folate concentration and accumulation analyses

Whole cell and mitochondrial folate concentrations were quantified using the *Lactobacillus casei* microbiological assay as previously described [37]. Mitochondrial cell fractions were isolated using Qproteome® Mitochondria Kit (Qiagen) following manufacturer's instructions. Total folates were normalized to protein concentrations for each sample [36].

HAP1 cell and *Δ*SHMT2 cell were plated in modified medium containing 0-nM (6S)-5-formyl-THF. After 48 h, medium was changed to modified medium containing labeled 25-nM (6S)-[$^{3}$H]5-formyl-THF. After 26 h, tritium in whole cells or mitochondrial samples isolated using a Qproteome® Mitochondria Kit (Qiagen) was quantified in a scintillation counter and normalized to protein concentrations.

#### Serine isotope tracer analysis

The flux of 1C units into the de novo dTMP synthesis pathway was quantified as previously described [38, 39]. $_{L}$-[2,3,4-$^{2}H_{3}$]-serine (250 μM) and leucine (26 mg/L) were supplemented into the HAP1 cell and *Δ*SHMT2 cell modified medium [38, 39]. Medium was changed every 2 days, and cells were harvested when they reached confluency. Total genomic DNA was isolated with the Roche High Pure PCR Template Preparation Kit per manufacturers' protocol, and DNA was dried and stored in a desiccator until analyses.

#### Mitochondrial DNA content, membrane potential, and mitochondrial function

Total genomic DNA was isolated with the Roche High Pure PCR Template Preparation Kit per manufacturers' protocol. Mitochondrial DNA copy number was determined by real-time quantitative PCR (Roche LightCycler® 480) as previously described [40], using LightCycler® 480 SYBR Green I Master (Roche) and 15 ng of DNA per reaction. Oligonucleotide primers for mouse Mito are as follows: (F 5′-CTAGAAACCCCGAAACCAAA and R 5′-CCAGCTATCACCAAGCTCGT and mouse B2M (F 5′-ATGGGAAGCCCGAACATACTG

and R 5′-CAGTCTCAGTGGGGGTGAAT (Integrated DNA Technologies).

The mitochondrial membrane potential was determined using JC-1 dye (Cayman) following the manufacturer's instructions. J-aggregate (excitation/emission = 535/595 nm) and monomer (excitation/emission = 484/535 nm) fluorescence were measured with a SpectraMax M3 (Molecular Devices).

The mitochondrial function was measured using a Seahorse XFe24 Extracellular Flux Analyzer (Agilent Technologies). Cells were cultured in the experimental 25- and 0-nM folate conditions for 4 doublings and then seeded in the same medium and allowed to adhere for 24 h. Basal respiration, ATP production, and extracellular acidification rate were determined following the manufacturer's instructions for the Cell Mitochondrial Stress Test (Agilent Technologies) and normalized to total cell count.

### Pyruvate kinase enzyme activity

HAP1 cells, ΔSHMT2 cells, and MEF cells were washed with 1 × PBS, pH 7.4, and then incubated with lysis buffer (50-mM Tris–HCl, pH 7.5, 1-mM EDTA, 150-mM NaCl, 1-mM DTT, protease inhibitor cocktail) for 15 min on ice to lyse cells. Protein was quantified by a BCA protein assay (Pierce), and 8 µg of fresh cell lysate was loaded per reaction following the instructions of the pyruvate kinase enzyme activity assay [41]. Optical absorbance of the reaction at 340 nm was measured every 15 s for 10 min with a SpectraMax M3 (Molecular Devices).

### Mitochondrial mass and NAD/NADH ratio

The mitochondrial mass was determined using a Citrate Synthase Activity Assay Kit (Sigma-Aldrich) following the manufacturer's instructions. Number of mitochondria was normalized to the total protein concentration. The NAD/NADH ratio was determined using a NAD/NADH-Glo Assay (Promega) according to the manufacturer's instructions. NAD/NADH ratio was normalized to total cell number determined by Hoechst 33,342 (Life Technologies) staining as described above.

### Statistical analyses

JMP® Pro statistical software version 15 (SAS Institute Inc.) was used for all statistical analyses. Linear mixed-effect models with main effects of media, genotype, and time (with time as a continuous variable), and all 2- and 3-way interactions, were used to determine HAP1 and ΔSHMT2 cell proliferation. For analyses in which HAP1 and ΔSHMT2 cells or *Shmt2*$^{+/+}$ and *Shmt2*$^{+/-}$ MEF cells were cultured in 25- or 0-nM folate supplemented medium, results were analyzed by two-way ANOVA with Tukey post hoc analysis to determine genotype by medium interaction and main effects of medium and genotype. For analyses in which HAP1 and ΔSHMT2 cells or *Shmt2*$^{+/+}$ and *Shmt2*$^{+/-}$ MEF cells were compared, results were analyzed by Student's *t*-test. All statistics were performed at the 95% confidence level ($\alpha = 0.05$), and groups were considered significantly different when $p \leq 0.05$. Descriptive statistics were calculated on all variables to include means and standard deviations.

#### Abbreviations

| | |
|---|---|
| dTMP | Thymidine monophosphate |
| FD | Folate deficient |
| FOCM | Folate-mediated one-carbon metabolism |
| GAPDH | Glyceraldegyde-3 phosphate dehydrogenase |
| IMDM | Iscove's modification of DMEM |
| MEF | Murine embryonic fibroblast |
| MEM | Minimal essential medium |
| mtDNA | Mitochondrial DNA |
| PKM1 | Pyruvate kinase M1 |
| OCR | Oxygen consumption rate |
| PKM2 | Pyruvate kinase M2 |
| PGC1α | PPARγ coactivator-1α |
| SHMT2 | Serine hydroxymethyltransferase 2 |
| THF | Tetrahydrofolate |

## Supplementary Information

The online version contains supplementary material available at https://doi.org/10.1186/s12263-023-00724-3.

**Additional file 1: Figure S1.** Cellular proliferation in HAP1 and ΔSHMT2 cells cultured in IMDM medium. Formate supplemented medium has no impact on rescuing the impaired cellular proliferation in ΔSHMT2 cells. Cell proliferation rates of ΔSHMT2 cells were compared with HAP1 cells by co-staining cells with Hoechst 33342 (to identify all cells) and propidium iodide (to identify dead cells). Fold change of each group was calculated by dividing by day 0 cell number. Data represent means ± SD values. Values represent $n = 6$ replicates of cell lines cultured in folate-sufficient IMDM medium. A) Cell proliferation rate and cell proliferation rate in the presence of 2 mM formate and B) relative day quantitation cell proliferation rate in the presence of 2 mM formate. Linear mixed-effects models with main effects of media, genotype, and time (with time as a continuous variable), and 2- and 3-way interactions were used to determine cell proliferation with a statistical significance at $p < 0.05$. Two-way ANOVA with Tukey's post-hoc analysis was used to determine media by genotype interaction and main effects of media and genotype with a statistical significance at $p < 0.05$ were used to analyze individual day proliferation. Levels not connected by the same letter are significantly different.

#### Acknowledgements

NA.

#### Authors' contributions

JLF and MSF designed research. JLF, JEB, KEH, and LFC conducted research. JLF and MSF analyzed data. JLF prepared the figures. JLF and MSF prepared the manuscript. MSF has primary responsibility for the final content. All authors reviewed and approved the final manuscript.

#### Funding

This study was financially supported by a President's Council of Cornell Women Award and supported by National Science Foundation Graduate Research Fellowship Program grant DGE-1650441 (to JEB).

#### Availability of data and materials

All data generated or analyzed during this study are included in this published article (and its supplementary information files).

## Declarations

**Ethics approval and consent to participate**
All mice were maintained under specific pathogen-free conditions in accordance with standard of use protocols and animal welfare regulations. All study protocols were approved by the Institutional Animal Care and Use Committee of Cornell University.

**Consent for publication**
NA.

**Competing interests**
The authors declare no competing interests.

**Author details**
[1]Division of Nutritional Sciences, Cornell University, Ithaca, NY, USA. [2]Department of Food, Nutrition, and Packaging Sciences, Clemson University, Clemson, SC 29634, USA. [3]Department of Chemical Engineering, Stanford University, Stanford, CA, USA. [4]Department of Cell, Developmental and Integrative Biology, University of Alabama at Birmingham, Birmingham, AL, USA.

Received: 8 April 2022 Accepted: 14 March 2023
Published online: 24 March 2023

**References**

1. Tibbetts AS, Appling DR. Compartmentalization of mammalian folate-mediated one-carbon metabolism. Annu Rev Nutr. 2010;30:57–81.
2. Xiu Y, Field MS. The roles of mitochondrial folate metabolism in supporting mitochondrial DNA synthesis, oxidative phosphorylation, and cellular function. Curr Dev Nutr. 2020;4:nzaa153 Oxford University Press.
3. Lan X, Field MS, Stover PJ. Cell cycle regulation of folate-mediated one-carbon metabolism. Wiley Interdiscip Rev Syst Biol Med. 2018;10(6):e1426.
4. De Koning TJ, Snell K, Duran M, Berger R, Poll-The BT, Surtees R. L-serine in disease and development. Biochem J. 2003;371:653–61.
5. Anderson DD, Quintero CM, Stover PJ. Identification of a de novo thymidylate biosynthesis pathway in mammalian mitochondria. Proc Natl Acad Sci U S A. 2011;108(37):15163–8.
6. Spizzichino S, Boi D, Boumis G, Lucchi R, Liberati FR, Capelli D, et al. Cytosolic localization and in vitro assembly of human de novo thymidylate synthesis complex. FEBS J. 2021;289(6):1625–49.
7. Xiu Y, Field MS. The roles of mitochondrial folate metabolism in supporting mitochondrial DNA synthesis, oxidative phosphorylation, and cellular function. Curr Dev Nutr. 2020;4(10):153.
8. García-Cazorla À, Verdura E, Juliá-Palacios N, Anderson EN, Goicoechea L, Planas-Serra L, et al. Impairment of the mitochondrial one-carbon metabolism enzyme SHMT2 causes a novel brain and heart developmental syndrome. Acta Neuropathol. 2020;140(6):971–5.
9. Majethia P, Bhat V, Yatheesha BL, Siddiqui S, Shukla A. Second report of SHMT2 related neurodevelopmental disorder with cardiomyopathy, spasticity, and brain abnormalities. Eur J Med Genet. 2022;65(6):104481.
10. Yang X, Wang Z, Li X, Liu B, Liu M, Liu L, et al. Shmt2 desuccinylation by SIRT5 drives cancer cell proliferation. Cancer Res. 2018;78(2):372–86.
11. Lee GY, Haverty PM, Li L, Kljavin NM, Bourgon R, Lee J, et al. Comparative oncogenomics identifies psmb4 and shmt2 as potential cancer driver genes. Cancer Res. 2014;74(11):3114–26.
12. Hashizume O, Ohnishi S, Mito T, Shimizu A, Iashikawa K, Nakada K, et al. Epigenetic regulation of the nuclear-coded GCAT and SHMT2 genes confers human age-associated mitochondrial respiration defects. Sci Rep. 2015;5(1):1–11.
13. Anderson DD, Woeller CF, Chiang EP, Shane B, Stover PJ. Serine hydroxymethyltransferase anchors de novo thymidylate synthesis pathway to nuclear lamina for DNA synthesis. J Biol Chem. 2012;287(10):7051–62.
14. Crott JW, Choi SW, Branda RF, Mason JB. Accumulation of mitochondrial DNA deletions is age, tissue and folate-dependent in rats. Mutat Res. 2005;570(1):63–70.
15. Chial H, Craig J. mtDNA and mitochondrial diseases. Nat Educ. 2008;1(1):217.
16. Bratic A, Larsson NG. The role of mitochondria in aging. J Clin Investig. 2013;123(3):951–7.
17. Fiddler JL, Xiu Y, Blum JE, Lamarre SG, Phinney WN, Stabler SP, et al. Reduced Shmt2 expression impairs mitochondrial folate accumulation and respiration, and leads to uracil accumulation in mouse mitochondrial DNA. J Nutr. 2021;151(10):2882–93.
18. Nadalutti CA, Ayala-Peña S, Santos JH. Mitochondrial DNA damage as driver of cellular outcomes. Am J Physiol Cell Physiol. 2022;322(2):C136–50.
19. Tani H, Ohnishi S, Shitara H, Mito T, Yamaguchi M, Yonekawa H, et al. Mice deficient in the Shmt2 gene have mitochondrial respiration defects and are embryonic lethal. Sci Rep. 2018;8(1):1–8.
20. Vigelsø A, Andersen NB, Dela F. The relationship between skeletal muscle mitochondrial citrate synthase activity and whole body oxygen uptake adaptations in response to exercise training. Int J Physiol Pathophysiol Pharmacol. 2014;6(2):84.
21 Field MS, Kamynina E, Chon J, Stover PJ. Nuclear folate metabolism. Annu Rev Nutr. 2018;38:219–43.
22. Kim D, Fiske BP, Birsoy K, Freinkman E, Kami K, Possemato R, et al. SHMT2 drives glioma cell survival in the tumor microenvironment but imposes a dependence on glycine clearance. Nature. 2015;520(7547):363–7.
23. Lucas S, Chen G, Aras S, Wang J. Serine catabolism is essential to maintain mitochondrial respiration in mammalian cells. Life Sci Alliance. 2018;1(2):e201800036.
24. Meiser J, Tumanov S, Maddocks O, Labuschagne CF, Athineos D, Van Den Broek N, et al. Serine one-carbon catabolism with formate overflow. Sci Adv. 2016;2(10):e1601273.
25. Taniguchi K, Sakai M, Sugito N, Kuranaga Y, Kumazaki M, Shinohara H, et al. PKM1 is involved in resistance to anti-cancer drugs. Biochem Biophys Res Commun. 2016;473(1):174–80.
26. Lunt SY, Muralidhar V, Hosios AM, Israelsen WJ, Gui DY, Newhouse L, et al. Pyruvate kinase isoform expression alters nucleotide synthesis to impact cell proliferation. Mol Cell. 2015;57(1):95–107.
27. Taniguchi K, Sakai M, Sugito N, Kuranaga Y, Kumazaki M, Shinohara H, et al. PKM1 is involved in resistance to anti-cancer drugs. Biochem Biophys Res Commun. 2016;473(1):174–80.
28. Lunt SY, Muralidhar V, Hosios AM, Israelsen WJ, Gui DY, Newhouse L, et al. Pyruvate kinase isoform expression alters nucleotide synthesis to impact cell proliferation. Mol Cell. 2015;57(1):95–107.
29. Chen L, Liu H, Ji Y, Ma Z, Shen K, Shangguan X, et al. Downregulation of SHMT2 promotes the prostate cancer proliferation and metastasis by inducing epithelial-mesenchymal transition. Exp Cell Res. 2022;415(2):113138.
30. Morscher RJ, Ducker GS, Li SHJ, Mayer JA, Gitai Z, Sperl W, et al. Mitochondrial translation requires folate-dependent tRNA methylation. Nature. 2018;554(7690):128–32.
31. Balsa E, Perry EA, Bennett CF, Jedrychowski M, Gygi SP, Doench JG, et al. Defective NADPH production in mitochondrial disease complex I causes inflammation and cell death. Nat Commun. 2020;11(1):1–12.
32. Minton DR, Nam M, McLaughlin DJ, Shin J, Bayraktar EC, Alvarez SW, et al. Serine catabolism by SHMT2 is required for proper mitochondrial translation initiation and maintenance of formylmethionyl-tRNAs. Mol Cell. 2018;69(4):610–21.
33. Liang H, Ward WF. PGC-1 alpha: a key regulator of energy metabolism. Adv Physiol Educ. 2006;30(4):145–51.
34. Goffart S, Wiesner RJ. Regulation and co-ordination of nuclear gene expression during mitochondrial biogenesis. Exp Physiol. 2003;88(1):33–40 Cambridge University Press.
35. Jin X, Li L, Peng Q, Gan C, Gao L, He S, et al. Glycyrrhetinic acid restricts mitochondrial energy metabolism by targeting SHMT2. iScience. 2022;25(5):104349.
36. Bensadoun A, Weinstein D. Assay of proteins in the presence of interfering materials. Anal Biochem. 1976;70(1):241–50.
37. Horne DW, Patterson D. Lactobacillus casei microbiological assay of folic acid derivatives in 96-well microtiter plates. Clin Chem. 1988;34(11):2357–9.
38. Herbig K, Chiang EP, Lee LR, Hills J, Shane B, Stover PJ. Cytoplasmic serine hydroxymethyltransferase mediates competition between folate-dependent deoxyribonucleotide and S-adenosylmethionine biosyntheses. J Biol Chem. 2002;277(41):38381–9.

39. Field MS, Kamynina E, Watkins D, Rosenblatt DS, Stover PJ. Human mutations in methylenetetrahydrofolate dehydrogenase 1 impair nuclear de novo thymidylate biosynthesis. Proc Natl Acad Sci U S A. 2015;112(2):400–5.
40. Malik AN, Czajka A, Cunningham P. Accurate quantification of mouse mitochondrial DNA without co-amplification of nuclear mitochondrial insertion sequences. Mitochondrion. 2016;29:59–64.
41. Teslaa T, Teitell MA. Techniques to monitor glycolysis. In: Methods in Enzymology. 2014. p. 91–114.

## Publisher's Note